Experimental and Molecular Pathology **71,** 40–54 (2001)
doi:10.1006/exmp.2001.2380, available online at http://www.idealibrary.com on IDEAL®

Atherosclerotic Lesions Are Associated with Increased Immunoreactivity for Inducible Nitric Oxide Synthase and Endothelin-1 in Thoracic Aortic Intimal Cells of Hyperlipidemic Watanabe Rabbits

Gjumrakch Aliev,*,†,‡ Mark A. Smith,§ Mark Turmaine,¶ Maxwell Lewis Neal,† Tatiana V. Zimina,* Robert P. Friedland,† George Perry,§ Joseph C. LaManna,† and Geoffrey Burnstock,¶,[1]

**Laboratory of Electron Microscopy, †Department of Neurology, ‡Department of Anatomy and Neuroscience, and §Institute of Pathology, School of Medicine, Case Western Reserve University, 10900 Euclid Avenue, Cleveland, Ohio 44106-4938; and ¶Autonomic Neuroscience Institute, Royal Free and University College Medical School, London NW3 2PF, United Kingdom*

Received February 14, 2001

The development and progression of atherosclerotic lesions in Watanabe heritable hyperlipidemic rabbits is associated with increases in inducible nitric oxide synthase (NOS2) and endothelin-1 (ET-1) immunoreactivity. In contrast, there is a reduction of immunoreactivity for neuronal NOS (NOS1) in aortic endothelial cells, but no change in endothelial NOS (NOS3) immunoreactivity. However, subendothelial macrophages and smooth muscle showed a different pattern of immunoreactivity of NADPH-diaphorase (NADPH-d), NOS2, ET-1, and NOS1. The lipid-rich macrophages in the intima were positively labeled for NADPH-d, NOS1, NOS2, NOS3, and ET-1. Smooth muscle cells in the subendothelium and the medial layers of the vascular wall were also positive for these markers. These results are consistent with the reduction of endothelium-dependent vasorelaxation that is known to occur during the development and progression of atherosclerosis in familial hypercholesterolemia. The data suggest a key role for vasoactive substances in the development of atherosclerosis.

Key Words: atherosclerosis; NADPH-diaphorase; neuronal nitric oxide synthase; endothelial nitric oxide synthase; inducible nitric oxide synthase; endothelin-1.

[1]To whom correspondence should be addressed at Autonomic Neuroscience Institute, Royal Free and University College Medical School, Rowland Hill Street, London NW3 2PF, UK. Fax: +44 20 7830 2949. E-mail: g.burnstock@ucl.ac.uk.

INTRODUCTION

Atherosclerotic lesions can alter vascular responses to stimuli in humans and other animals (Verbeuren *et al.*, 1986, 1990; Bossaller *et al.*, 1987; Forstermann *et al.*, 1988; Kolodgie *et al.*, 1990; Lefer and Sedar, 1991; Cirillo *et al.*, 1992; Ragazzi *et al.*, 1993). Endothelium-dependent and endothelium-independent relaxation can be reduced in atherosclerotic arteries while vasoconstrictor responses can be enhanced. These modifications in vascular reactivity vary considerably among the different models of atherosclerosis and with the degree of hypercholesterolemia and genetic status (Verbeuren *et al.*, 1986, 1990, 1994).

Nitric oxide (NO) has been identified as the main endothelium-derived relaxing factor (EDRF). NO is synthesized from L-arginine by NO synthase (NOS) by vascular endothelial cells (ECs) (Palmer *et al.*, 1987; Verbeuren *et al.*, 1994). Constitutive NOS (neuronal and endothelial specific, or NOS1 and NOS3, respectively) and inducible NOS (macrophage specific or NOS2) isoforms of NOS have been demonstrated in the endothelium (Moncada *et al.*, 1991; Dusting,

0014-4800/01 $35.00

1995). Injuries (e.g., mechanical, chemical, viral, or bacterial) to the vascular system cause the release of mediators such as interleukin-1 and tumor necrosis factor α by inflammatory cells. These mediators induce NOS2 in most vascular cells (e.g., macrophages, ECs, smooth muscle cells, and fibroblasts) (Dusting, 1995; Nathan and Xie, 1994). Chronic inhibition of NO production accelerates neointima formation and impairs endothelial function in hypercholesterolemic rabbits (Cooke *et al.*, 1992; Cayatte *et al.*, 1994; Tsao *et al.*, 1994). This neointima formation impairs the NO- and prostacyclin-mediated vasodilator function of ECs (De *et al.*, 1991, 1992; Arthur *et al.*, 1994). In addition, endogenous NO may modulate endothelial–monocyte interaction (Tsao *et al.*, 1994, 1996; Zeiher *et al.*, 1995), which plays an important role in the suppression of vascular adhesion molecule-1 (Tsao *et al.*, 1996). ECs synthesize, store, and release a number of other vasoactive substances including endothelin-1 (ET-1) (Yanagisawa *et al.*, 1988; Lerman *et al.*, 1990; Tsao *et al.*, 1996), a process that inhibits NO. However, the exact role of NO and ET-1 in the pathogenesis of atherosclerosis remains unclear and controversial. The balance of the EDRF/NO–ET system may play a crucial role in vascular homeostasis especially during cardiac allograft rejection (Szabolcs *et al.*, 1996), congestive heart failure (Xie *et al.*, 1996), cardiomyopathy (De *et al.*, 1993), postischemic vascular injury (Verbeuren *et al.*, 1990; Kubes *et al.*, 1991; Niu *et al.*, 1996), and atherogenesis (Lerman and Burnett, 1992; Aliev *et al.*, 2000), after long-term sympathectomy (Aliev *et al.*, 1996), and in the development of vascular diseases, such as hypertension (Watts *et al.*, 1994; Wennmalm, 1994; White *et al.*, 1994), as well as during normal aging processes (Loesch *et al.*, 1991; Aliev *et al.*, 1995; Loesch and Burnstock, 1995).

Changes in the endothelial content of NOS and ET-1 could occur in the development of atherosclerotic lesions before visible ultrastructural or functional changes to the endothelium are detected. Little is known about the ultrastructural distribution of different isoforms of NOS (NOS1, NOS2, and NOS3) and ET-1 during the development and progression of atherosclerosis and their relationship to NADPH-diaphorase (NADPH-d) histochemical activity. In the present study we used Watanabe heritable hyperlipidemic (WHHL) rabbits as a model for the study of human familial hypercholesterolemia (Buja *et al.*, 1983). We investigated the influence of atherosclerotic lesions on NADPH-d histochemistry, NOS1, NOS2, NOS3, and ET-1 immunoreactivity in intimal cells of the thoracic aorta (Aliev *et al.*, 1993). Pre- and postembedding electron microscopy (EM), immunocytochemistry, and NADPH-d histochemistry were used for qualitative and quantitative analyses.

MATERIALS AND METHODS

Animals. Male WHHL and New Zealand White rabbits (NZW; newborn, 3–6 months, 12 months, and 24 months of age; five animals for each age group) were obtained from the animal facility of Southampton University. All animals received the same standard laboratory diet and water *ad libitum*.

Perfusion fixation. Rabbits, under terminal anesthesia, were perfused retrogradely via the abdominal aorta with Medium 199 containing 10 IU/ml heparin for 1 min and then perfusion fixed with 0.1 M cacodylate buffer containing 4% paraformaldehyde and 0.1% glutaraldehyde at pH 7.3 (Aliev *et al.*, 1993, 1995, 2000) according to the BHF and NIH guidelines for the use of animals in research. The thoracic aorta was dissected and immersion fixed for 4–6 h at 4°C with the same fresh fixative solution. Finally, aortic tissues were transferred to cacodylate buffer and stored overnight at 4°C. The aorta was sectioned to produce 6- to 8-mm-long strips that were then processed for NADPH-d histochemistry and for pre- and postembedding EM immunocytochemistry.

NADPH-d histochemistry. Strips of aorta for NADPH-d staining were incubated with 1.2 mM β-NADPH, 0.24 M nitroblue tetrazolium, 15.2 mM L-malic acid, and 0.01% Triton X-100 or 0.01% Tween 20 in 0.1 M Tris HCl (pH 7.4) at 37°C for 100 min. Aortic tissues were then washed in Tris buffer four times for 10 min. Samples were then processed for standard EM procedure. Semithin sections for preliminary light microscopy analysis were stained with toluidine blue. Randomly selected ultrathin sections were stained with uranyl acetate and lead citrate and studied using a Jeol TEM-1010 or Jeol 1200 CX microscope operating at 80 kV. Control tissues were processed using the same procedure but without β-NADPH or nitroblue tetrazolium.

Preembedding immunocytochemistry. Immunocytochemistry of NOS1, NOS2, NOS3, and ET-1 in thoracic aortic tissues was performed using the peroxidase–anti-peroxidase (PAP) method as previously reported (Aliev *et al.*, 1995, 2000). Briefly, samples were exposed to 0.3% H_2O_2 in 50% methanol for 30 min and washed in 0.1 M Tris buffer (Tris), pH 7.4. Samples were then exposed to normal goat serum (NGS) diluted 1:40 in Tris containing sodium azide and bovine albumin for 1.5 h and rinsed in Tris solution. Samples were incubated for 48 h at 4°C with monoclonal antibody for NOS2 (1:500), NOS3 (1:1000), or rabbit antibody for NOS1 or ET-1 (1:1000) in Tris containing sodium azide and bovine albumin. The specimens were then washed in Tris and exposed to goat anti-mouse or goat anti-rabbit

immunoglobulin G serum (IgG; mono- or polyclonal antibodies, respectively) diluted 1:40 in Tris with sodium azide and bovine albumin for 1.5 h. The specimens were then washed in Tris and exposed to a monoclonal mouse or polyclonal rabbit PAP complex diluted 1:60 in Tris for 3 h. After exposure to 3′,3′-diaminobenzidine and H_2O_2, the specimens were washed in Tris and postfixed with 2.5% glutaraldehyde in cacodylate buffer overnight. Samples were then processed for standard EM procedure (Aliev *et al.*, 1993, 1995, 1996, 2000). Semithin sections for preliminary light microscopic analysis were stained with 1% toluidine blue. Ultrathin sections for immunocytochemistry were stained with uranyl acetate and lead citrate and investigated using a Jeol TEM-1010 or Jeol TEM 1200 EX microscope.

Postembedding double gold labeling immunocytochemistry. Strips of aorta (osmicated or nonosmicated) were dehydrated in ethanol and propylene oxide and embedded in Unicryl. Localization of NOS1 (10 or 20 nm), NOS2 (10 nm), NOS3 (10 nm), and ET-1 (10 or 20 nm) in aortic wall cells was examined in ultrathin sections of the specimens (on uncoated nickel grids) utilizing the immunogold labeling techniques reported previously (Loesch *et al.*, 1991; Aliev *et al.*, 1996). The procedure was as follows: sections were (1) exposed to 5% H_2O_2 solution at room temperature for 15 min; (2) washed five times in twice-distilled water at 5-min intervals; (3) incubated with hot inactivated NGS (1:10) in Tris buffer with 0.5% bovine albumin serum, 0.1% Tween 20, 0.9% NaCl, and 0.1% sodium azide (pH 8.0); (4) washed five times with buffer solution every 20 min; (5) incubated with primary antibody to NOS1, or NOS2, or NOS3 (dilution 1:300–400) overnight at 4°C in Tris buffer; (6) washed with Tris buffer five times every 20 min; (7) incubated at room temperature for 3–4 h with goat anti-rabbit (for NOS1) or goat anti-mouse IgG (for NOS2 or NOS3) serum-coated colloidal gold probe coupled to 10-nm gold particles at a dilution of 1:75–90 in Tris buffer; (8) washed five times with Tris buffer containing Tween 20 every 20 min; (9) washed five times with twice-distilled water every 20 min. The same procedure was used for second labeling with polyclonal antibody against NOS1 or ET-1. Polyclonal antibody specimens were incubated with hot inactivated NGS diluted in the same Tris buffer. Dilution of primary antibody for second labeling was 1:200. The concentration of goat anti-rabbit IgG serum-coated colloidal gold particles was 1:50–60. Other steps of the immunogold labeling procedure were as above. Finally, after several further washings with Tris and twice-distilled water, specimens were stained with uranyl acetate and lead citrate and examined using a transmission electron microscope.

Controls for pre- and postembedding immunocytochemistry. Monoclonal antibody against NOS2 was purchased from Transduction Laboratories (Lexington, KY). The specificity and characteristics for the monoclonal antibody against NOS3 (H-32) antibody have been reported previously (Pollock *et al.*, 1993; Aliev *et al.*, 1996, 2000). Rabbit polyclonal antiserum against NOS1 was obtained from Abbot Laboratories (Chicago, IL). The characteristics of this antibody have also been reported (Aliev *et al.*, 1995; Loesch and Burnstock, 1995). Rabbit antiserum against human ET-1 was purchased from Sigma (St. Louis, MO) and the specificity has been demonstrated recently (Aliev *et al.*, 1995, 2000; Loesch *et al.*, 1991; Loesch and Burnstock, 1995). Specificity control included the omission of primary antibodies and the IgG step and the preabsorption of the antiserum with synthetic peptides corresponding to the antigen. The control procedure for PAP was similar to that described above.

In preliminary experiments, we tested the specificity of consecutive double labeling gold techniques (Aliev *et al.*, 1996; Loesch and Burnstock, 1995). The single and double labeling for different antibodies was also tested using different sizes of gold particles (10 and 20 nm). The specificity of face A and B of sections was also tested. Moreover, some grids were incubated with mixed antibody (NOS2 or NOS3 in combination with another polyclonal antibody: NOS2 and ET-1; NOS3 and ET-1; NOS2 and NOS1; NOS3 and NOS1). The density of gold particles for different vasoactive substances was the same for double labeling (data not shown). After the stabilization of double labeling, postembedding double gold immunocytochemistry procedures were generally used. Control specimens were exposed to the same procedure, after the omission of primary antibody or by incubation with a synthetic antibody.

Morphometric measurements. The number of ECs positive or negative for NADPH-d, NOS1, NOS2, NOS3, and ET-1 were counted in ultrathin sections taken from at least 5 different levels of each specimen from five rabbits in each age group (Aliev *et al.*, 1995, 2000; Loesch and Burnstock, 1995). The percentage of ECs positively stained for NADPH-d was calculated for each rabbit. When examined with an EM, ECs were counted on randomly selected areas.

The specific volume of gold particles (number of gold particles per square micrometer) in ECs for antibodies against NOS1, NOS2, NOS3, and ET-1 was evaluated by counting gold granules and tissue points from randomly selected photographic fields (100 observations from each of the five animals used per age group) as reported previously (Aliev *et al.*, 1996).

Statistical analysis. All values were expressed as mean ± SEM of n observations. Two-way analysis of variance

was used to analyze results from repeated measurements. End-point experiments were tested for analysis of variance. This was followed by a least significant difference procedure (SPSS, Inc.) to determine the significance of differences between groups. *P* values of less than 0.05 were considered statistically significant.

RESULTS

NADPH-d histochemistry. NADPH-d histochemical staining was observed in the membrane and cytoplasm of the granular endoplasmic reticulum of ECs from NZW (Fig. 1a) and WHHL rabbits (Table 1), comparable to the first description of electron microscope immunolocalization of NADPH-d in endothelial cells (Loesch *et al.*, 1993). However, the NADPH-d histochemical reaction was seen in medial layers of thoracic aorta only in WHHL rabbits with atherosclerotic lesions, but not in nonlesioned aortic wall of WHHL or in NZW control rabbits. The structures of atherosclerotic lesions in the vascular wall of WHHL rabbits that showed the most intense NADPH-d histochemical reactions were in subendothelial macrophage foam cells or smooth muscle cells (SMCs), particularly in the late stages of atherosclerotic lesion (12- and 24-month-old groups) (Table 1). NADPH-d reactivity was also seen in perivascular nerves in atherosclerotic lesions of thoracic aorta in WHHL rabbits, especially in the 24-month-old group, but was not present in nonlesioned aorta from WHHL or in control NZW rabbits. There is an age-related change in the percentage of NADPH-d positively stained ECs from NZW and WHHL rabbits. Less NADPH-d-positive staining was observed in older groups of NZW and WHHL rabbits (Table 1). However, lipid-laden areas of the cytoplasm were negative for NADPH-d. As a negative control, no staining was found in NZW and WHHL rabbits without NADPH-d or nitroblue tetrazolium (Fig. 1b).

Preembedding PAP immunocytochemistry: NOS1 and NOS3. Immunostaining for the antibodies against NOS1 and NOS3 in ECs of newborn to 24-month-old rabbits showed that the number of NOS1 immunopositive ECs gradually decreased with age in WHHL, but showed no change in NZW rabbits (Table 2). In NZW (Figs. 2a and 2b) and WHHL rabbits (Figs. 2d, 3a, and 3b) immunopositive staining for both NOS1 and NOS3 was seen in the cytoplasm of aortic ECs, but not in the nucleus or in most other organelles like mitochondria and vesicles (Fig. 2b). NOS1 immunoreactivity was found in cells of the intima and medial layers of atherosclerotic lesions in the aorta of WHHL rabbits (Fig. 2d). The intensity of NOS1 immunoreactivity correlated with the degree of atherosclerotic lesion, but lipid-laden areas of the cytoplasm were always free from immunopositive precipitate (Fig. 2d). In contrast, immunopositive staining was only localized in thoracic aorta ECs of NZW rabbits. In WHHL rabbits, NOS3 immunostaining was unchanged during the development of atherosclerotic lesions (Table 2). However, in ECs with dystrophic changes, the intensity of NOS3 immunostaining decreased and was very often absent (Figs. 3a, and 3b). NOS3 immunostaining was frequently seen in the cytoplasm of subendothelial macrophages and/or SMC (Fig. 3b). In control specimens where the primary antibody was omitted, no immunopositive reaction was present in the cytoplasm of ECs, in the nuclei, or in any other layer of the thoracic aortic wall in NZW or WHHL rabbits (Fig. 2c).

Preembedding PAP immunocytochemistry: NOS2. Only in newborn NZW rabbits did ECs show a slight immunopositive reaction for the antibody against NOS2 (data not shown). However, in WHHL rabbits, aortic intima showed an immunopositive reaction for NOS2 in EC of all age groups (Fig. 4; Table 2). During aging, the intensity and the number of NOS2 immunopositive EC increased (Table 2), but in ECs with dystrophic changes there was an absence of immunoreactivity to NOS2 (Fig. 4c). However, NOS2 immunoreactivity was observed in subendothelial lipid-laden macrophages and SMCs (Figs. 4c and 4d). The cytoplasm of SMC in medial layers of aorta with atherosclerotic lesions also showed high immunopositive staining for NOS2. Lipid-containing areas of the cytoplasm were free from immunopositive precipitate. In control specimens no immunopositive reaction was seen after omission of the primary antibody.

Preembedding PAP immunocytochemistry: ET-1. In NZW rabbits the ultrastructural distribution of ET-1-immunopositive ECs was unchanged across age groups. In mature WHHL rabbits, there was threefold more ET-1-immunopositive ECs than in NZW rabbits of corresponding age (Table 2). The ultrastructural distribution of ET-1 immunoreactivity during aging in NZW (Figs. 5a and b) and WHHL rabbits was generally similar to that of the NOS immunostaining.

In further advanced atherosclerotic lesions, aortic wall cells, including ECs and other intimal cells, showed increased ET-1 immunoreactivity. Moreover, in 24-month-old WHHL rabbits "*whole*" ET-1-immunopositive ECs were often seen (Fig. 5d). Increased ET-1 immunoreactivity in the aortic intimal cells of atherosclerotic lesions, but not lipid-containing areas of the cytoplasm, was observed. Often, "islands" of ET-1-immunopositive precipitate were observed

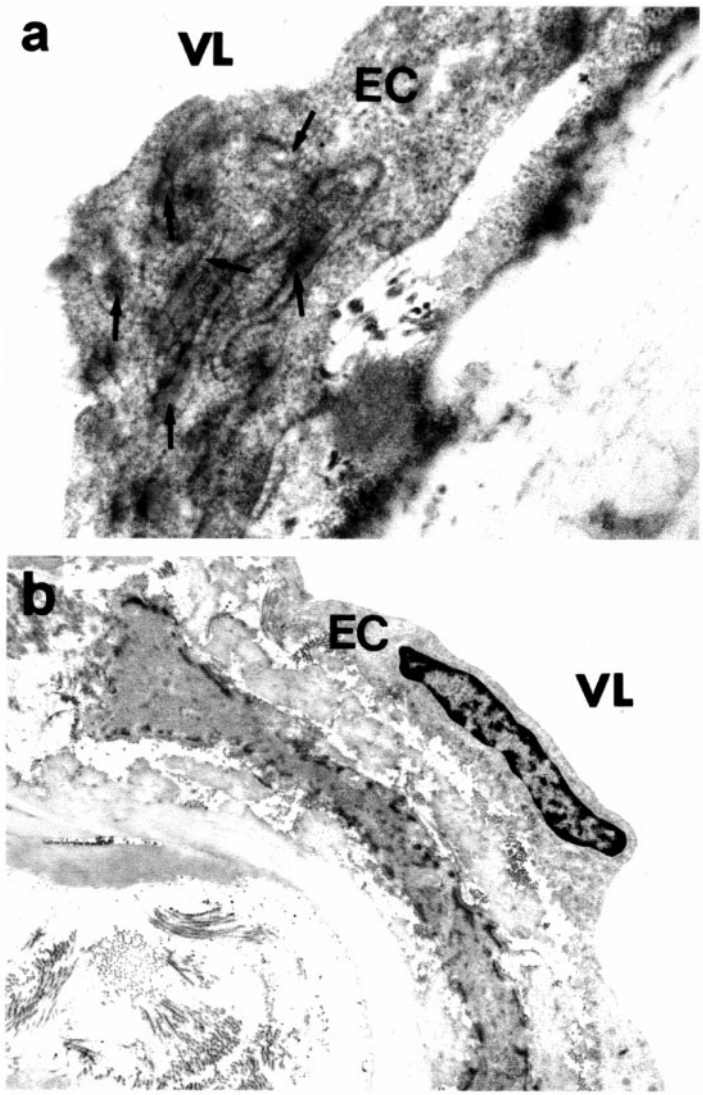

FIG. 1. NADPH-diaphorase histochemical staining characteristics of the thoracic aortic endothelium from 12-month-old NZW rabbits. (a) NADPH-d reaction seen in the membrane and in the cytoplasm of the granular endoplasmic reticulum (arrows) of an endothelial cell (EC). Original magnification ×40,000. (b) Section from aorta showing the absence of any histochemical reaction when samples were subjected to the same procedure but incubated without NADPH-d. Original magnification ×12,000. VL, vessel lumen.

in the subendothelium. The lesioned SMC from medial layers of the aortic wall also showed an intense ET-1-immunopositive reaction in their matrices.

No immunopositive reaction was observed in control specimens after the omission of antibody or with absorption of a synthetic peptide corresponding to the antigen in aortic wall cells (Figs. 5c and 5e).

Postembedding electron microscopy double gold labeling cytochemistry. ECs from NZW rabbit aorta of all age groups showed a large number of gold particles (10 or 20 nm) in the cytoplasm when stained for NOS1. NOS1-containing gold particles were seen in the external membrane and in the cytoplasm of the granular endoplasmic reticulum and mitochondria.

In WHHL rabbits the number of NOS1-containing gold particles appeared to decrease with age (Figs. 6d and 6e; Table 3). Often no NOS1 gold particles, or only a few, were observed in the cytoplasm of ECs of 12- or 24-month-old

TABLE 1

The Percentage of NADPH-d-Positive Endothelial Cells (EC) in Thoracic Aortic Endothelium from WHHL and NZW Rabbits in Different Age Groups

	Percentage of EC-positive staining for NADPH-d			
	Newborn	3–6 months	12 months	24 months
WHHL	90–95	75–80	85–90	80–85
NZW	80–90	70–75	80–85	50–55

Note. One hundred random observations were made from each of five rabbits ($n = 5$).

WHHL rabbits. However, in the aortic intima where subendothelial macrophages or SMC were present, NOS1 was prominent in cytoplasm (Fig. 6e), although the lipid-laden areas of the cytoplasm were free from NOS1.

Only aortic EC from newborn NZW rabbits showed the presence of NOS2 in the cytoplasm (Fig. 6b; Table 3). In aging rabbits NOS2 was reduced and was very often completely absent.

The ultrastructural distribution of NOS2-positive gold particles in WHHL rabbits was similar to that for NOS1. The particles were associated with the cytoplasm rather than with cell organelles. In particular, EC and subendothelial macrophages or SMCs from aorta of 24-month-old WHHL rabbits showed an increased amount of NOS2 in the cytoplasm. A cluster-like localization of NOS2 was prevalent (Fig. 6e). The subendothelial lipid-laden macrophages and SMC in areas of atherosclerotic lesions showed clusters of NOS2 in their cytoplasm, but not in lipid-containing areas of the cell.

NOS3 (10 nm) distribution remained generally unchanged across the newborn to 24-month-old NZW and WHHL age groups. Similar to NOS1 and NOS2, NOS3 was distributed throughout the cytoplasm, and a few gold particles were closely associated with cytoplasmic organelles. Some ECs showed clusters of NOS3 in their matrices (Fig. 6d). During the progression of atherosclerotic lesions, large numbers of NOS3-containing gold particles were seen in the cytoplasm of subendothelial macrophages and lipid-laden SMC. Additionally, as seen with the NOS1 and NOS2 procedures, lipid-containing areas of the cytoplasm were devoid of any gold particles.

In NZW rabbits, ET-1 (20 nm) was randomly distributed throughout the cytoplasm, and in 24-month-old animals the number was considerably higher compared with young NZW rabbits (Fig. 6b). ECs from the thoracic aorta of WHHL rabbits from all age groups showed a distribution of ET-1 similar to that of NOS2 and NOS3, but not NOS1 (see Fig. 6). The usual localization of ET-1 was cluster-type. During the progression of atherosclerotic lesions, ET-1 in the aortic wall cells sharply increased (Fig. 6e). These increases were particularly more evident in areas of atherosclerotic lesion of the intima, mainly in regions where lipid-laden macrophages and SMCs were present in the subendothelium. ET-1 was also seen in cytoplasmic parts of EC, which sharply protruded into the vessel lumen. However, in atherosclerotic lesions where dystrophic changes in EC occur, a decrease or an absence of ET-1 was frequently observed. The density of ET-1-containing gold particles in subendothelial lipid-laden macrophages and SMCs increased with the progression of atherosclerotic lesions.

Control specimens, which were processed according to the same procedure, but with the omission of primary antibodies (NOS1-3 or ET-1) or with synthetic peptides, were devoid of any gold particles in their cytoplasm. No particles were seen in the nuclei of EC or in other layers of the vascular wall in NZW and WHHL rabbits using the control methods. Only very occasionally were one or two gold particles found when rabbit polyclonal antibodies were used (data not shown).

Morphometric studies: Preembedding PAP immunocytochemistry. The difference between NZW and WHHL rabbits in the number of ECs positively stained for NOS1, NOS2, and ET-1, but not NOS3, was significant across all

TABLE 2

The Percentage of Endothelial Cells Immunopositive for the Different Isoforms of NOS or ET-1 in WHHL and Control NZW Rabbits from the Different Age Groups

	Percentage of ECs immunopositive for NOS isoforms or ET-1			
	Newborn	3–6 months	12 months	24 months
NOS1				
WHHL	15–20	10–15	5–8	<1
NZW	20–25	15–20	8–10	8–10
NOS2				
WHHL	20–25	25–30	35–40	45–50
NZW	<1	0	0	0
NOS3				
WHHL	30–40	40–50	55–60	40–45
NZW	50–65	65–80	60–70	45–50
ET-1				
WHHL	15–20	25–30	45–50	65–75
NZW	15–20	8–10	10–15	20–25

Note. One hundred random observations were made from each rabbit (5 rabbits in each age group were used).

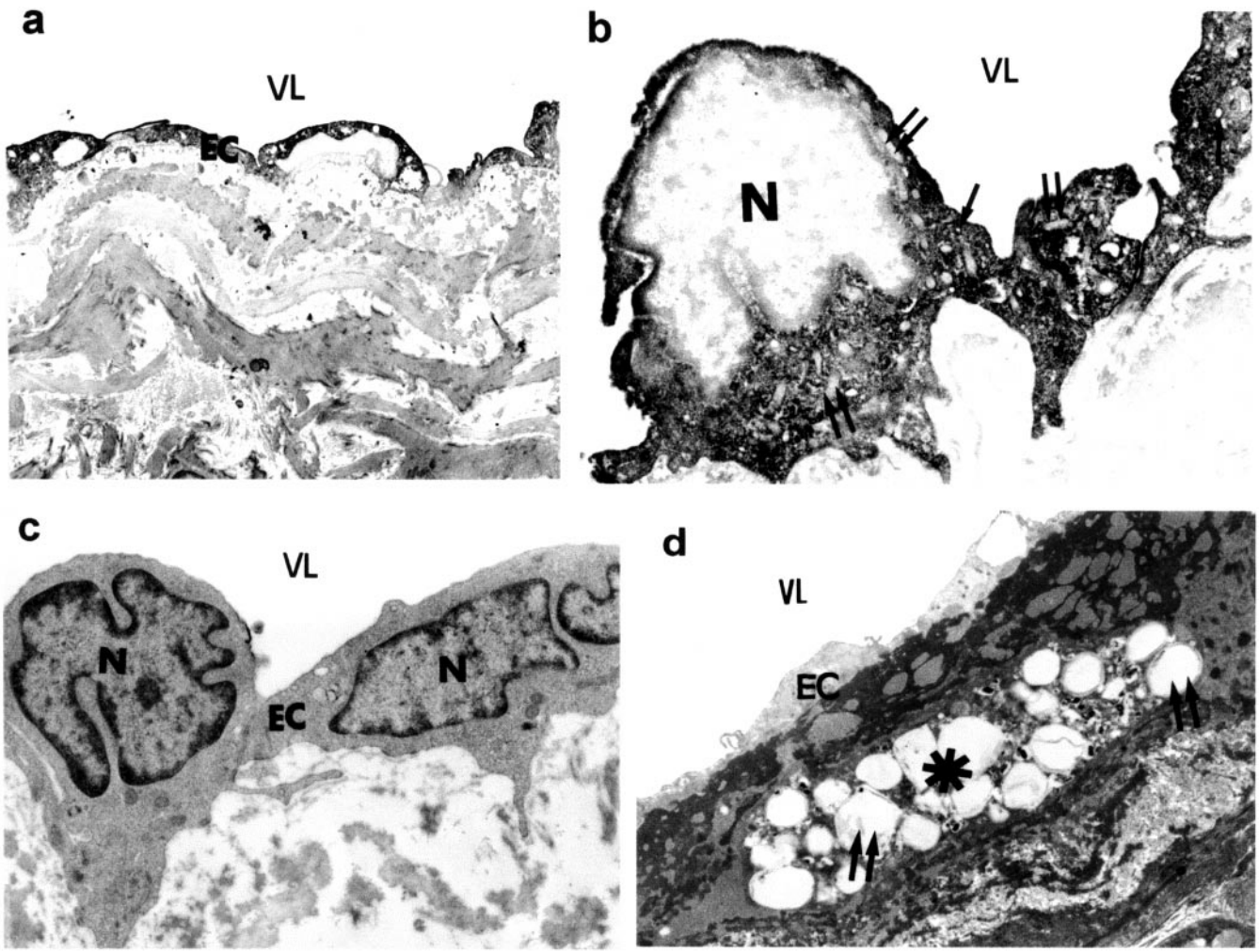

FIG. 2. NOS1 and NOS3 labeling in the thoracic aortic intima of NZW rabbits from the different age groups (a, b) and control specimen (c) and NOS1 labeling in the thoracic aortic intimal cells of 12-month-old WHHL rabbit (d). (a) A large number of NOS1 immunopositive endothelial cells (EC) were seen in the thoracic aortic intima from 12-month-old NZW rabbits. Original magnification ×2500. (b) A high intensity of NOS3 immunopositive reaction in the cytoplasm of EC was seen in the thoracic aortic intima from 6-month-old NZW rabbit. Most cytoplasmic vesicles (single arrow) and mitochondria (double arrows) and the nucleus (N) of EC were free from NOS3 immunopositive precipitate. Original magnification ×10,000. (c) Thoracic aorta from 12-month-old NZW rabbit, processed for immunocytochemistry as a control by omitting NOS3 antibody, showing no immunopositive staining in EC or in the subendothelium. Original magnification ×10,000. (d) Thin section obtained from aorta of 12-month-old WHHL rabbit. NOS1 immunopositive macrophages appear in atherosclerotic lesioned aorta (asterisk). Lipid-laden areas of the cytoplasm were free from immunopositive products (double arrows). EC does not show any NOS1 immunopositive reaction. Original magnification ×5000. VL, vessel lumen.

age groups (Table 2). The percentage of NOS1-positive ECs was 15–20 and 20–25% in newborn WHHL and NZW rabbits, respectively. During the progression of atherosclerotic lesions the number of NOS1-immunopositive ECs decreased with age. In the 24-month-old rabbits, less than 1% of ECs were immunopositive for the antibody against NOS1 (Table 2). In aged control NZW rabbits the proportion of NOS1-immunopositive ECs was unchanged compared with the 12-month-old rabbits (8–10%). However, the percentage of NOS1-immunopositive ECs was significantly lower than that found in NZW newborns (20–25%).

The number of NOS3-immunopositive ECs in WHHL rabbits remained generally unchanged during the progression of atherosclerotic lesions. Moreover, in 24-month-old

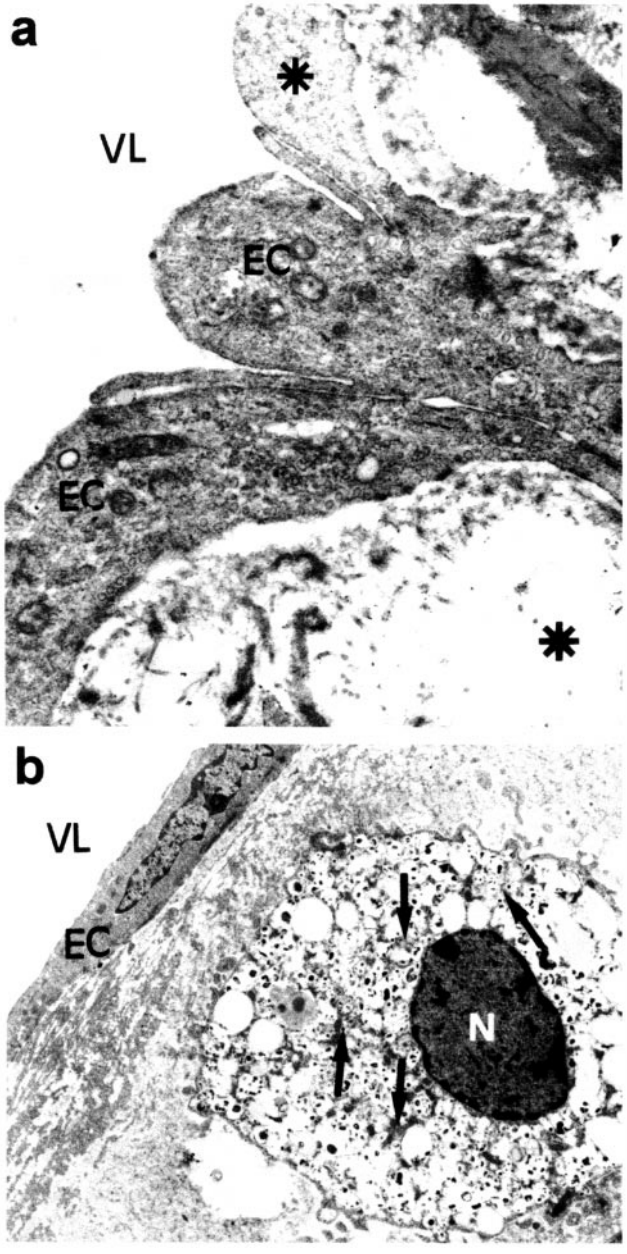

FIG. 3. Ultrastructural features of NOS3 immunolabeling in thoracic aortic intima of WHHL rabbits. (a) NOS3 immunopositive endothelial cells (EC) in thoracic aorta from 12-month-old WHHL rabbit. Immunopositive staining is absent in one EC and in subendothelium (asterisks). Original magnification ×15,000. (b) High intensity of NOS3 immunopositive staining in the cytoplasm of the subendothelial macrophages (arrows). Immunopositive staining was absent in EC and in lipid-laden areas of macrophages. Original magnification ×4000. VL, vessel lumen; N, nucleus.

WHHL rabbits the number of NOS2- and NOS3-immunopositive ECs was similar (Table 2). The number of ET-1-positive ECs in NZW rabbits decreased from newborn to 3–6 months and in 12-month-old rabbits, but subsequently returned to the level seen in newborn animals (Table 2). In WHHL rabbits the number of ET-1-immunopositive ECs was significantly increased from newborn to 24 months, when 65–75% were ET-1-positive. The number of ET-1-immunopositive lipid-laden macrophages and SMCs in the intima and medial layers of the vascular wall also showed a significant increase during the progression of atherosclerotic lesions (data not shown).

Quantitative postembedding double gold labeling immunocytochemistry. Gold particles associated with NOS1, NOS2, NOS3, and ET-1 in thoracic aortic EC of WHHL and NZW rabbits at different ages are summarized in Table 3.

The presence of NOS1-containing gold particles in newborn WHHL rabbits was slightly, but not significantly, less than in newborn NZW rabbits. However, in 3- to 6-month-old WHHL rabbits a significant decrease in specific volume of gold particles was seen when compared with control NZW rabbit aortic endothelium ($P < 0.05$; Table 3). No significant difference in the specific volume of NOS1-containing gold particles was observed between WHHL and NZW rabbits in the 12-month-old groups. In 24-month-old WHHL rabbits, however, aortic ECs showed significantly less NOS1 compared with NZW rabbits at the same age ($P < 0.05$; Table 3). We have found that from newborn to 24 months there is a statistically significant decrease in the amount of NOS1 in aortic ECs of WHHL rabbits. Significant decreases were also seen between 12 and 24 months ($P < 0.05$). In NZW rabbits, significant decreases in the number of NOS1-containing positive gold particles were seen between newborn and 12 and 24 months. Significant differences were also observed between the following: 3–6 months and 12 months, 3–6 months and 24 months, 12 months and 24 months (Table 3).

The number of NOS2-labeled gold particles in newborn, 3- to 6-month, 12-month, and 24-month-old WHHL rabbits was significantly higher than in NZW rabbits at corresponding ages ($P < 0.05$; Table 3). During the progression of atherosclerotic lesions, NOS2-positive gold particles increased with aging, but significant differences were seen only between newborns and two other groups: 3- to 6-month-old and 24-month-old rabbits ($P < 0.05$; Table 3). There were no significant differences observed in NOS3 levels in aortic ECs between newborn and 24-month-old WHHL and NZW rabbits (Table 3). However, there were significant

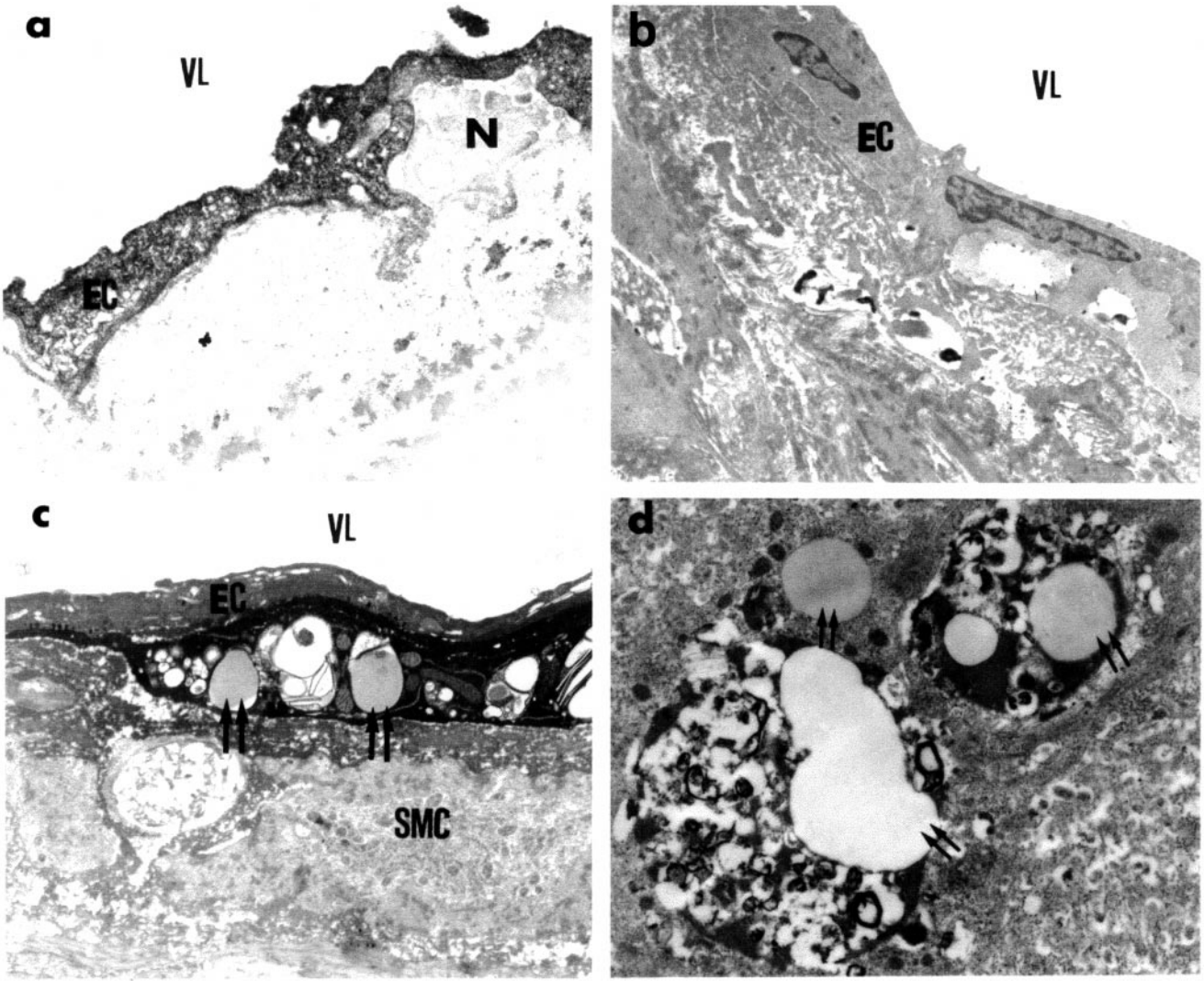

FIG. 4. The ultrastructural characteristics of NOS2 staining on thoracic aorta from WHHL rabbits during the progression of atherosclerotic lesions. (a) NOS2 immunopositive staining in endothelial cells (EC) from the thoracic aorta of 6-month-old WHHL rabbit. Original magnification ×10,000. (b) NOS2 immunopositive staining is absent in the control specimen processed for immunocytochemistry but omitting NOS2 antibody. Section was obtained from thoracic aorta of 24-month-old WHHL rabbit. Original magnification ×6000. (c) and (d) The presence of NOS2 immunopositive macrophages in the subendothelium of thoracic aorta from 1- and 24-month-old WHHL rabbits, respectively. No immunopositive staining is seen in the cytoplasm of altered endothelium. The lipid-laden area of the cytoplasm of the macrophages also shows the absence of any NOS2 immunopositive reaction (double arrows). Original magnification ×8,000 (c), ×10,000 (d). N, nucleus; SMC, smooth muscle cell; VL, vessel lumen.

differences between the 3- to 6-month-old and the 12-month-old WHHL and NZW rabbit groups ($P < 0.05$). No significant differences were seen between the different age groups of WHHL rabbits, except between the 3- to 6-month-old and the 12-month-old groups ($P < 0.05$; Table 3).

In NZW rabbits, the number of NOS3-positive gold particles was significantly higher in newborn, 3–6, and 12 months of age than in 24-month-old animals (Table 3). Thoracic aortic ECs of 3- to 6-month-old NZW rabbits showed significantly less NOS3 compared with the 12-month-old group, but their volume was significantly more than that seen at 24 months ($P < 0.05$). Significant difference was also seen between the 12- and 24-month-old groups ($P < 0.05$; Table 3).

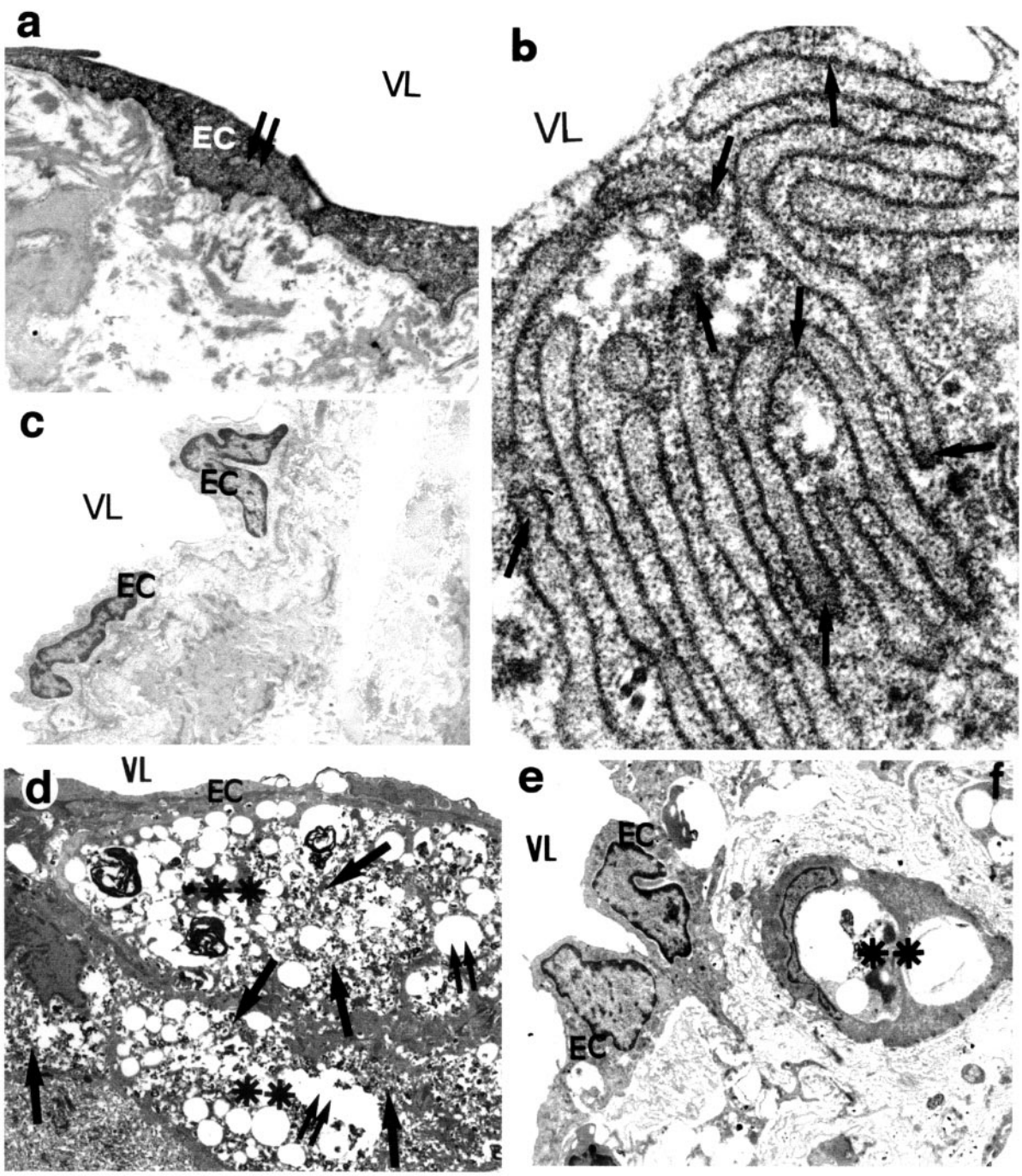

FIG. 5. Ultrastructural features of ET-1 labeling in thoracic aortic endothelial cells (EC) from NZW rabbits and WHHL rabbits of differing ages. (a) A high intensity of ET-1 immunopositive EC was seen in thoracic aortic intima in 6-month-old NZW rabbit. ET-1 immunopositive reaction is absent in the matrix of mitochondria (double arrows) and EC nucleus (N). Original magnification ×8000. (b) An intense ET-1 immunopositive reaction (arrows) was seen in the cytoplasm of "synthetic" types of EC from newborn NZW rabbits. The membrane and the matrix of granular endoplasmic reticulum displayed a particularly intense immunopositive reaction. Original magnification ×40,000. (c) Control specimen of aorta from 12-month-old NZW rabbit, processed using the same procedures but omitting ET-1 antibody. No immunopositive reaction was seen in EC or other areas of aortic intima. Original magnification ×6000. (d) ET-1 immunopositive subendothelial macrophages (double asterisks; arrows indicate the immunopositive precipitate) in thoracic aortic cells of a 24-month-old WHHL rabbit. Immunopositive staining is absent in altered EC and lipid-enriched areas of the cytoplasm of subendothelial macrophages (double arrows). Original magnification ×3000. (e) Thoracic aortic intimal cells were free from any ET-1 immunopositive reaction when samples were processed after omission of ET-1 antibody (double asterisk indicates the subendothelial foam cells). Original magnification ×5000. VL, vessel lumen.

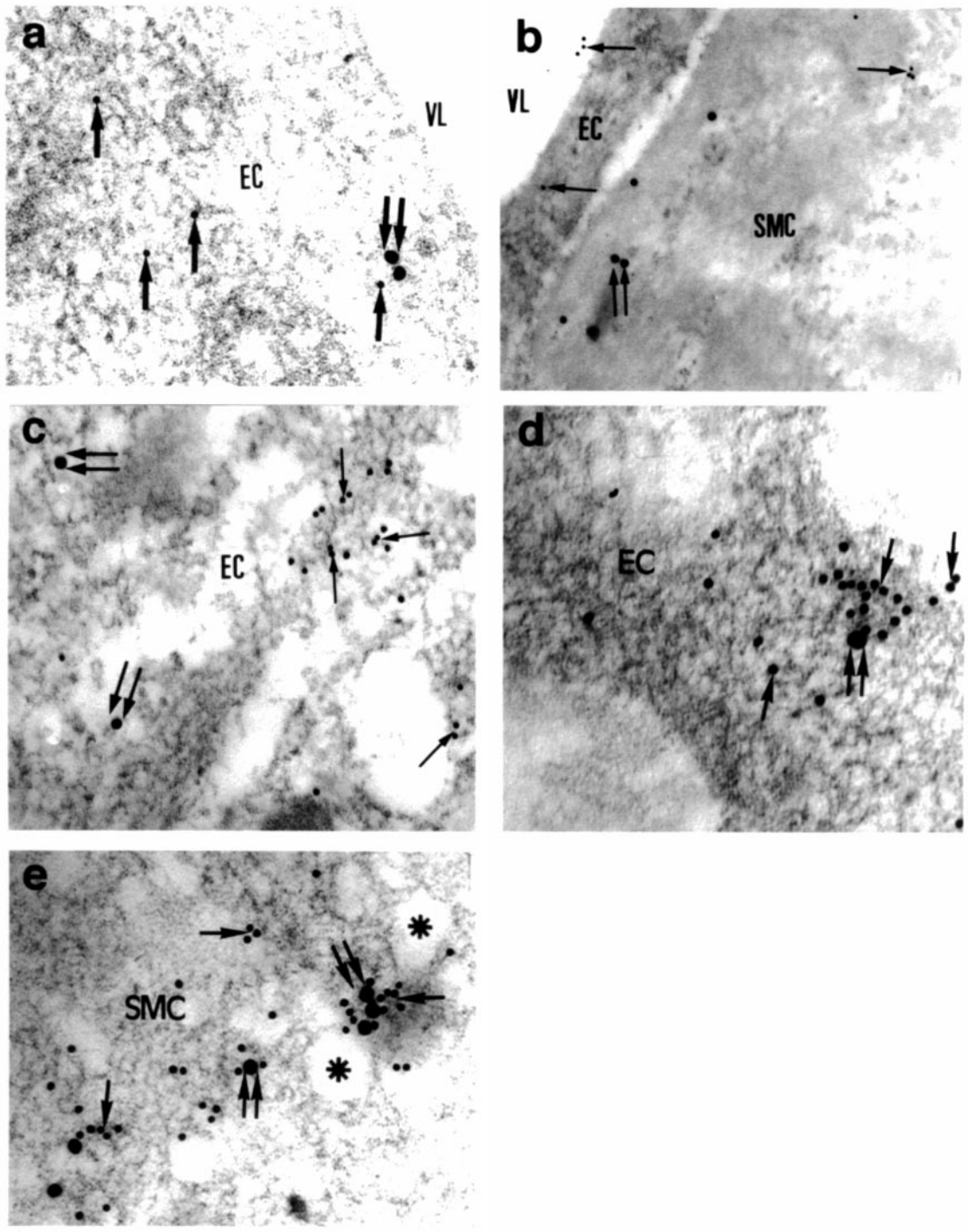

FIG. 6. Ultrastructural features of the distribution of gold particles containing NOS1, NOS2, NOS3, and ET-1 in thoracic aortic endothelium using the postembedding double goldlabeling techniques. (a) Endothelial cell (EC) from 12-month-old NZW rabbit showing gold particles labeling NOS3 (10-nm particles; single arrows), but not ET-1 (20-nm particles; double arrows), distributed throughout the cytoplasm. Original magnification ×100,000. (b) Thoracic aorta from newborn NZW rabbit shows the presence of a few NOS2-positive gold particles (10 nm) in the cytoplasm of EC (arrows). NOS2 and ET-1 immunopositive gold particles (20 nm, double arrow) were mostly seen in the cytoplasm of smooth muscle cells (SMC) in medial layers. Original magnification ×50,000. (c) Clusters of NOS2-positive gold particles (10 nm, single arrows) seen in the cytoplasm

TABLE 3

The Effects of Atherosclerotic Lesion Development on the Specific Volume of Gold Particles (Number of Gold Particles/EC μm^2) Labeled with the Different NOS Isoforms and ET-1 in Thoracic Aortic EC from WHHL and NZW Rabbits

	Number of gold particles/EC μm^2			
	Newborn	3–6 months	12 months	24 months
NOS1				
WHHL	0.65 ± 0.02	0.35 ± 0.03*·†	0.27 ± 0.02*·†·¶	0.11 ± 0.002*·‡·†·#
NZW	0.71 ± 0.01	0.68 ± 0.04¶	0.32 ± 0.01‡·†·¶	0.41 ± 0.004‡·†·#
NOS2				
WHHL	0.72 ± 0.01*	0.76 ± 0.03*·¶	0.91 ± 0.08*	0.99 ± 0.003*·†
NZW	0.01 ± 0.02	0.0001 ± 0.001†	0	0
NOS3				
WHHL	0.93 ± 0.02	0.97 ± 0.001*·#	1.2 ± 0.08*	0.96 ± 0.02
NZW	1.01 ± 0.008	1.4 ± 0.007†	1.61 ± 0.01†·‡·¶	0.99 ± 0.005‡
ET-1				
WHHL	0.92 ± 0.009*	0.79 ± 0.02*·†·#·¶	1.1 ± 0.04*·‡	1.29 ± 0.03*·†
NZW	0.81 ± 0.006	0.69 ± 0.007†·#·¶	0.83 ± 0.01¶	0.89 ± 0.002†·#

Note. Statistical differences ($P < 0.05$) are denoted by: *compared with control (NZW at corresponding age); †compared with newborn; ‡compared with 3–6 months; #compared with 12 months; ¶compared with 24 months. All values are expressed as means ± SEM.

The increase in ET-1 containing positive gold particles in WHHL rabbits was significantly more than that seen in NZW rabbits across age groups (Table 3). Comparative analysis showed that significant differences were seen between the following age groups: newborn and 24 months, 3–6 months and 12 months, and 12- and 24-month-old WHHL rabbits (Table 3). In NZW rabbits ET-1 decreased from newborn to 3–6 months and had increased by 12 and 24 months. However, the significant differences were seen only between newborn and 3–6 months and 24-month-old groups; 3–6 months compared with 12 months, 3–6 months compared with 24 months; and 12 compared with 24 months (Table 3; $P < 0.05$, respectively).

DISCUSSION

The present study shows that there are significant increases in the expression of NADPH-d and NOS1, NOS2, NOS3, and ET-1 immunoreactivity in aortic intimal cells and medial layers. A significant decrease in NOS1, but not in NOS3 immunoreactivity is limited to thoracic aortic ECs of WHHL rabbits and is associated with the progression of atherosclerotic lesions. The lack of changes in these vasoactive substances in early stages of atherosclerotic lesions indicates that the influence of high lipid plasma levels and a deficiency of low-density lipoprotein receptors among EC in aortic intima is a long-term effect. These findings suggest that high lipid levels selectively influence the vasoactive substances in the rabbit thoracic aortic endothelium and other intimal cells. Alternatively, the atherosclerotic lesions may modulate the endothelium-dependent vasorelaxation and vasoconstrictor activity in EC during their development and progression.

Selective decrease of endothelium-dependent vasorelaxation has been reported in the pulmonary artery and aorta of cholesterol-fed rabbits (Verbeuren *et al.*, 1986, 1990, 1994), in the thoracic aorta (Kolodgie *et al.*, 1990; Ragazzi *et al.*, 1993, 1995), peripheral large arteries and hindlimb microcirculation of WHHL rabbits (Cirillo *et al.*, 1992), and in human

of EC from the thoracic aorta of newborn WHHL rabbits (double arrows indicate ET-1 immunopositive gold particles, 20 nm). Original magnification ×80,000. (d) Thoracic aorta from 12-month-old WHHL rabbit. Note the presence of a greater number of NOS3-positive gold particles (10 nm, single arrows) compared with NOS1 (20 nm, double arrow) in the EC. Original magnification ×120,000. (e) The cytoplasm of the subendothelial SMC of the thoracic aorta from a 24-month-old WHHL rabbit shows clusters of NOS1- (20 nm, double arrows) and NOS2- (10 nm, single arrows) positive gold particles. Lipid-laden areas of the cytoplasm were free from gold particles (asterisks). Original magnification ×100,000. VL, vessel lumen.

coronary arteries (Bossaller *et al.*, 1987; Forstermann *et al.*, 1988). Reduced synthesis and/or inactivation of EDRF have been implicated in impaired endothelium-dependent vasorelaxation in WHHL rabbits (Tagawa *et al.*, 1991). The vascular content of L-arginine is significantly lower in WHHL rabbits than in NZW rabbits (Chinellato *et al.*, 1992). However, later studies have shown that the NOS3 protein and mRNA increase in WHHL rabbit atherosclerotic aorta despite impaired endothelium-dependent vasorelaxation (Kanazawa *et al.*, 1996).

The absence of differences in positive staining for NADPH-d in ECs of control and experimental groups suggests that all three isoforms of NOS utilize NADPH-d as a cofactor (Palmer *et al.*, 1988; Moncada *et al.*, 1991) and that the enzymatic activities of NOS and NADPH-d can be attributed to the same protein (Hope *et al.*, 1991). The chronic actions of high levels of plasma lipids also influence vasoactive substances of perivascular nerves. Some studies have shown that diet-induced atherosclerosis exerts an inhibitory action on the sympathetic nerve terminals in the aorta and pulmonary artery of the rabbit, and, together with an inhibitory effect at the postjunctional level, it results in a loss of responsiveness to nerve stimulation (Verbeuren *et al.*, 1994). Consistently, we have shown that increased ET-1 immunoreactivity in thoracic aortic endothelium in rats is associated with the depression of NOS3 immunoreactivity after long-term, but not short-term sympathectomy (Aliev *et al.*, 1996). It is possible that the inhibition of intraneuronal deamination could be the key factor in influencing the increases of NADPH-d and therefore NOS immunoreactivity in perivascular nerves seen in the thoracic aortic intimal cells in our experiments.

The expression of NOS1 immunoreactivity in the intimal cells of the thoracic aortic wall during the development of atherosclerotic lesions in WHHL rabbits is probably related to the formation of large amounts of reactive oxygen species (ROS) which require NO for their neutralization (White *et al.*, 1994). ROS have been implicated in both the pathogenesis and the altered physiological responses to atherosclerosis. Oxidation of low-density lipoproteins, a critical event in atheroma formation, is associated with enhanced cellular production of O^{2-}; (Steinberg *et al.*, 1989). The presence of different isoforms of NOS such as we observed in atherosclerotic aortic intimal cells may be related to the degradation of NO by ROS, which is formed continuously in the chronic hyperlipidemic condition. Rubanyi and co-workers have demonstrated that the continuous utilization of picomolar amounts of NO by constitutive types of NOS (NOS1 and NOS3) seen in various disease conditions is induced by impaired neutralization of unwanted ROS (Rubanyi and Vanhoutte, 1986; Rubanyi *et al.*, 1991). The decreased amount of vasoactive NO and the diminished response of endothelial cell dependant vasorelaxation could lead to the expression of inducible NOS, characterized by the formation of nanomolar amounts of NO (Buga *et al.*, 1993; Ignarro, 1990).

It has been shown that NO derived from intact endothelium under whole-blood arterial flow conditions may be an important modulator for neutrophil interaction with intact endothelium (Provost *et al.*, 1994). Increased NOS immunoreactivity in aortic wall cells probably exerts a protective effect by increasing the number of leukocytes adhered to vascular endothelium. The progression of atherosclerotic lesions in WHHL rabbits induces changes in NOS and ET-1 immunoreactivity, which starts at an early stage of embryogenesis. Subsequently, chronic accumulation of plasma lipids, adhesion and migration of monocytes from vessel lumen to vascular wall, and migration of SMCs from medial layers may stimulate expression of NOS in foam cells and SMCs of subendothelial and medial layers of the aortic wall. Expression of NOS2 plays a significant role in the control of major vessel and ductus arterious caliber in the rat fetus (Bustamante *et al.*, 1996). It has been shown that apoptosis of myocardial cells during cardiac allograft rejection parallels the expression of NOS2, suggesting that apoptosis can be triggered by NO and peroxynitrite (Szabolcs *et al.*, 1996). Reduced synthesis and/or inactivation of EDRF have been implicated in impaired endothelium-dependent relaxation in WHHL rabbits (Kolodgie *et al.*, 1990; Ragazzi *et al.*, 1993). Moreover, the atherosclerotic vessels become less sensitive to vasoactive stimuli (Kolodgie *et al.*, 1990). This may be due to thickened intima or increased lipids in the vessel wall of atherosclerotic vessels, which act as a barrier to diffusion of EDRF from the endothelium to the underlying vascular smooth muscle (De *et al.*, 1991, 1992).

The present study shows that during the development of atherosclerotic lesions in WHHL rabbits, NOS3 immunoreactivity remains unchanged. NOS3 is mainly a plasma membrane protein that metabolizes L-arginine to NO (Pollock *et al.*, 1993; Garcia-Cardena *et al.*, 1996; Aliev *et al.*, 2000). The absence of NOS3 immunoreactivity in damaged EC suggests different activities of vasoactive substances *in vivo* and *in vitro*. It is probably caused by altered intracellular trafficking of NOS3 proteins and NOS3-dependent NO release from EC, which are associated with the development and progression of atherosclerotic lesions.

In conclusion, the present study has demonstrated that the development and progression of atherosclerotic lesions in WHHL rabbits induce increased expression of NADPH-d, NOS2, and ET-1 immunoreactivity and no changes in NOS3

immunoreactivity, but selectively decreased NOS1 in aortic endothelial cells. These data suggest that the balance between vessel constrictors and relaxants play a key role in exacerbating atherosclerosis and impairment of the blood supply in regions of lesion.

ACKNOWLEDGMENTS

This study was supported by the British Heart Foundation. The authors thank Abbot Laboratories for providing the NOS1 and NOS3 antiserum and Mr. R. Jordan for editorial assistance.

REFERENCES

Aliev, G., Mironov, A., Cirillo, R., Mironov, A. J., Gorelova, E., and Prosdocimi, M. (1993). Evidence for the presence of early vascular lesions in newborn Watanabe heritable hyperlipidemic (WHHL) rabbits. *Atherosclerosis* **101,** 17–24.

Aliev, G., Miah, S., Turmaine, M., and Burnstock, G. (1995). An ultrastructural and immunocytochemical study of thoracic aortic endothelium in aged Sprague–Dawley rats. *J. Submicrosc. Cytol. Pathol.* **27,** 477–490.

Aliev, G., Ralevic, V., and Burnstock, G. (1996). Depression of endothelial nitric oxide synthase but increased expression of endothelin-1 immunoreactivity in rat thoracic aortic endothelium associated with long-term, but not short-term, sympathectomy. *Circ. Res.* **79,** 317–323.

Aliev, G., Shi, J., Perry, G., Friedland, R. P., and LaManna, J. C. (2000). Depression of constitutive nitric oxide synthase, but increased expression of inducible nitric oxide synthase and endothelin-1 immunoreactivity in aortic endothelial cells of Donryu rats on a cholesterol-enriched diet. *Anat. Rec.* **260,** 16–25.

Arthur, J. F., Dusting, G. J., and Woodman, O. L. (1994). Impaired vasodilator function of nitric oxide associated with developing neointima in conscious rabbits. *J. Vasc. Res.* **31,** 187–194.

Bossaller, C., Habib, G. B., Yamamoto, H., Williams, C., Wells, S., and Henry, P. D. (1987). Impaired muscarinic endothelium-dependent relaxation and cyclic guanosine 5′-monophosphate formation in atherosclerotic human coronary artery and rabbit aorta. *J. Clin. Invest.* **79,** 170–174.

Buga, G. M., Griscavage, J. M., Rogers, N. E., and Ignarro, L. J. (1993). Negative feedback regulation of endothelial cell function by nitric oxide. *Circ. Res.* **73,** 808–812.

Buja, L. M., Kita, T., Goldstein, J. L., Watanabe, Y., and Brown, M. S. (1983). Cellular pathology of progressive atherosclerosis in the WHHL rabbit. An animal model of familial hypercholesterolemia. *Life Sci.* **3,** 87–101.

Bustamante, S. A., Pang, Y., Romero, S., Pierce, M. R., Voelker, C. A., Thompson, J. H., Sandoval, M., Liu, X., and Miller, M. J. (1996). Inducible nitric oxide synthase and the regulation of central vessel caliber in the fetal rat. *Circulation* **94,** 1948–1953.

Cayatte, A. J., Palacino, J. J., Horten, K., and Cohen, R. A. (1994). Chronic inhibition of nitric oxide production accelerates neointima formation and impairs endothelial function in hypercholesterolemic rabbits. *Arterioscler. Thromb.* **14,** 753–759.

Chinellato, A., Ragazzi, E., Polverino, D. L., and Fassina, G. (1992). Reduced L-arginine/lysine and L-arginine/aspartic acid ratios in aorta from Watanabe heritable hyperlipidemic (WHHL) rabbit. *Pharmacol. Res.* **25,** 255–258.

Cirillo, R., Aliev, G., Italiano, G., and Prosdocimi, M. (1992). Functional responses of hindlimb circulation in aged normal and WHHL rabbits. *Atherosclerosis* **93,** 133–144.

Cooke, J. P., Singer, A. H., Tsao, P., Zera, P., Rowan, R. A., and Billingham, M. E. (1992). Antiatherogenic effects of L-arginine in the hypercholesterolemic rabbit. *J. Clin. Invest.* **90,** 1168–1172.

De, M. G., Bult, H., Van, H. A., Jordaens, F. H., Buyssens, N., and Herman, A. G. (1991). Neointima formation impairs endothelial muscarinic receptors while enhancing prostacyclin-mediated responses in the rabbit carotid artery. *Circ. Res.* **68,** 1669–1680.

De, M. G., Bult, H., and Herman, A. G. (1992). Selective muscarinic alterations of nitric oxide-mediated relaxations by neointima. *J. Cardiovasc. Pharmacol.* **20 (Suppl. 12),** S205–S207.

De, B. A., Radomski, M. W., Why, H. J., Richardson, P. J., Bucknall, C. A., Salas, E., Martin, J. F., and Moncada, S. (1993). Nitric oxide synthase activities in human myocardium. *Lancet* **341,** 84–85.

Dusting, G. J. (1995). Nitric oxide in cardiovascular disorders. *J. Vasc. Res.* **32,** 143–161.

Forstermann, U., Mugge, A., Alheid, U., Haverich, A., and Frolich, J. C. (1988). Selective attenuation of endothelium-mediated vasodilation in atherosclerotic human coronary arteries. *Circ. Res.* **62,** 185–190.

Garcia-Cardena, G., Oh, P., Liu, J., Schnitzer, J. E., and Sessa, W. C. (1996). Targeting of nitric oxide synthase to endothelial cell caveolae via palmitoylation: Implications for nitric oxide signaling. *Proc. Natl. Acad. Sci. USA* **93,** 6448–6453.

Hope, B. T., Michael, G. J., Knigge, K. M., and Vincent, S. R. (1991). Neuronal NADPH diaphorase is a nitric oxide synthase. *Proc. Natl. Acad. Sci. USA* **88,** 2811–2814.

Ignarro, L. J. (1990). Biosynthesis and metabolism of endothelium-derived nitric oxide. *Annu. Rev. Pharmacol. Toxicol.* **30,** 535–560.

Kanazawa, K., Kawashima, S., Mikami, S., Miwa, Y., Hirata, K., Suematsu, M., Hayashi, Y., Itoh, H., and Yokoyama, M. (1996). Endothelial constitutive nitric oxide synthase protein and mRNA increased in rabbit atherosclerotic aorta despite impaired endothelium-dependent vascular relaxation. *Am. J. Pathol.* **148,** 1949–1956.

Kolodgie, F. D., Virmani, R., Rice, H. E., and Mergner, W. J. (1990). Vascular reactivity during the progression of atherosclerotic plaque. A study in Watanabe heritable hyperlipidemic rabbits. *Circ. Res.* **66,** 1112–1126.

Kubes, P., Suzuki, M., and Granger, D. N. (1991). Nitric oxide: an endogenous modulator of leukocyte adhesion. *Proc. Natl. Acad. Sci. USA* **88,** 4651–4655.

Lefer, A. M., and Sedar, A. W. (1991). Endothelial alterations in hypercholesterolaemia and atherosclerosis. *Pharmacol. Res.* **23,** 1–12.

Lerman, A., and Burnett, J. C. J. (1992). Intact and altered endothelium in regulation of vasomotion. *Circulation* **86,** III12–III19.

Lerman, A., Hildebrand, F. L. J., Margulies, K. B., O'Murchu, B., Perrella, M. A., Heublein, D. M., Schwab, T. R., and Burnett, J. C. J. (1990). Endothelin: A new cardiovascular regulatory peptide. *Mayo Clin. Proc.* **65,** 1441–1455.

Loesch, A., and Burnstock, G. (1995). Ultrastructural localization of nitric oxide synthase and endothelin in coronary and pulmonary arteries of newborn rats. *Cell Tissue Res.* **279,** 475–483.

Loesch, A., Bodin, P., and Burnstock, G. (1991). Colocalization of endothelin, vasopressin and serotonin in cultured endothelial cells of rabbit aorta. *Peptides* **12,** 1095–1103.

Loesch, A., Belai, A., and Burnstock, G. (1993). Ultrastructural localization of NADPH-diaphorase and colocalization of nitric oxide synthase in endothelial cells of the rabbit aorta. *Cell Tissue Res.* **274,** 539–545.

Moncada, S., Palmer, R. M., and Higgs, E. A. (1991). Nitric oxide: Physiology, pathophysiology, and pharmacology. *Pharmacol. Rev.* **43,** 109–142.

Nathan, C., and Xie, Q. W. (1994). Regulation of biosynthesis of nitric oxide. *J. Biol. Chem.* **269,** 13725–13728.

Niu, X. F., Ibbotson, G., and Kubes, P. (1996). A balance between nitric oxide and oxidants regulates mast cell-dependent neutrophil–endothelial cell interactions. *Circ. Res.* **79,** 992–999.

Palmer, R. M., Ferrige, A. G., and Moncada, S. (1987). Nitric oxide release accounts for the biological activity of endothelium-derived relaxing factor. *Nature* **327,** 524–526.

Palmer, R. M., Ashton, D. S., and Moncada, S. (1988). Vascular endothelial cells synthesize nitric oxide from L-arginine. *Nature* **333,** 664–666.

Pollock, J. S., Nakane, M., Buttery, L. D., Martinez, A., Springall, D., Polak, J. M., Forstermann, U., and Murad, F. (1993). Characterization and localization of endothelial nitric oxide synthase using specific monoclonal antibodies. *Am. J. Physiol.* **265,** C1379–C1387.

Provost, P., Lam, J. Y., Lacoste, L., Merhi, Y., and Waters, D. (1994). Endothelium-derived nitric oxide attenuates neutrophil adhesion to endothelium under arterial flow conditions. *Arterioscler. Thromb.* **14,** 331–335.

Ragazzi, E., Chinellato, A., Pandolfo, L., Froldi, G., Caparrotta, L., Prosdocimi, M., Aliev, G., and Fassina, G. (1993). Atherosclerosis-related remodeling of aortic relaxation to purines in the Watanabe heritable hyperlipidemic rabbit. *J. Pharmacol. Exp. Ther.* **266,** 1091–1096.

Ragazzi, E., Chinellato, A., Pandolfo, L., Froldi, G., Caparrotta, L., Aliev, G., Prosdocimi, M., and Fassina, G. (1995). Endothelial nucleotide-mediated aorta relaxation in aged Watanabe heritable hyperlipidemic rabbits. *J. Cardiovasc. Pharmacol.* **26,** 119–126.

Rubanyi, G. M., and Vanhoutte, P. M. (1986). Superoxide anions and hyperoxia inactivate endothelium-derived relaxing factor. *Am. J. Physiol.* **250,** H822–H827.

Rubanyi, G. M., Ho, E. H., Cantor, E. H., Lumma, W. C., and Botelho, L. H. (1991). Cytoprotective function of nitric oxide: Inactivation of superoxide radicals produced by human leukocytes. *Biochem. Biophys. Res. Commun.* **181,** 1392–1397.

Steinberg, D., Parthasarathy, S., Carew, T. E., Khoo, J. C., and Witztum, J. L. (1989). Beyond cholesterol. Modifications of low-density lipoprotein that increase its atherogenicity. *N. Engl. J. Med.* **320,** 915–924.

Szabolcs, M., Michler, R. E., Yang, X., Aji, W., Roy, D., Athan, E., Sciacca, R. R., Minanov, O.P., and Cannon, P. J. (1996). Apoptosis of cardiac myocytes during cardiac allograft rejection. Relation to induction of nitric oxide synthase. *Circulation* **94,** 1665–1673.

Tagawa, H., Tomoike, H., and Nakamura, M. (1991). Putative mechanisms of the impairment of endothelium-dependent relaxation of the aorta with atheromatous plaque in heritable hyperlipidemic rabbits. *Circ. Res.* **68,** 330–337.

Tsao, P. S., McEvoy, L. M., Drexler, H., Butcher, E. C., and Cooke, J. P. (1994). Enhanced endothelial adhesiveness in hypercholesterolemia is attenuated by L-arginine. *Circulation* **89,** 2176–2182.

Tsao, P. S., Buitrago, R., Chan, J. R., and Cooke, J. P. (1996). Fluid flow inhibits endothelial adhesiveness. Nitric oxide and transcriptional regulation of VCAM-1. *Circulation* **94,** 1682–1689.

Verbeuren, T. J., Coene, M. C., Jordaens, F. H., Van, H. C., Zonnekeyn, L. L., and Herman, A. G. (1986). Effect of hypercholesterolemia on vascular reactivity in the rabbit. II. Influence of treatment with dipyridamole on endothelium-dependent and endothelium-independent responses in isolated aortas of control and hypercholesterolemic rabbits. *Circ. Res.* **59,** 496–504.

Verbeuren, T. J., Jordaens, F. H., Van, H. C., Van, H. A., and Herman, A. G. (1990). Release and vascular activity of endothelium-derived relaxing factor in atherosclerotic rabbit aorta. *Eur. J. Pharmacol.* **191,** 173–184.

Verbeuren, T. J., Simonet, S., and Herman, A. G. (1994). Diet-induced atherosclerosis inhibits release of noradrenaline from sympathetic nerves in rabbit arteries. *Eur. J. Pharmacol.* **270,** 27–34.

Watts, S. W., Finta, K. M., Lloyd, M. C., Storm, D. S., and Webb, R. C. (1994). Enhanced vascular responsiveness to Bay K 8644 in mineralocorticoid- and *N*-nitro arginine-induced hypertension. *Blood Press.* **3,** 340–348.

Wennmalm, A. (1994). Nitric oxide (NO) in the cardiovascular system: Role in atherosclerosis and hypercholesterolemia. *Blood Press.* **3,** 279–282.

White, C. R., Brock, T. A., Chang, L. Y., Crapo, J., Briscoe, P., Ku, D., Bradley, W. A., Gianturco, S. H., Gore, J., and Freeman, B. A. (1994). Superoxide and peroxynitrite in atherosclerosis. *Proc. Natl. Acad. Sci. USA* **91,** 1044–1048.

Xie, Y. W., Shen, W., Zhao, G., Xu, X., Wolin, M. S., and Hintze, T. H. (1996). Role of endothelium-derived nitric oxide in the modulation of canine myocardial mitochondrial respiration in vitro. Implications for the development of heart failure. *Circ. Res.* **79,** 381–387.

Yanagisawa, M., Kurihara, H., Kimura, S., Goto, K., and Masaki, T. (1988). A novel peptide vasoconstrictor, endothelin, is produced by vascular endothelium and modulates smooth muscle Ca^{2+} channels. *J. Hypertens. Suppl.* **6,** S188–S191.

Zeiher, A. M., Fisslthaler, B., Schray-Utz, B., and Busse, R. (1995). Nitric oxide modulates the expression of monocyte chemoattractant protein 1 in cultured human endothelial cells. *Circ. Res.* **76,** 980–986.